KfK 4122
August 1986

Bénard Convection in a Partly Solidified Two-Component System

G. Zimmermann, U. Müller, S. H. Davis
Institut für Reaktorbauelemente

Kernforschungszentrum Karlsruhe

KERNFORSCHUNGSZENTRUM KARLSRUHE
Institut für Reaktorbauelemente

KfK 4122

Bénard Convection in a Partly Solidified Two-Component System

G. Zimmermann, U. Müller,

S.H. Davis*)

*) Dept. of Engineering Sciences and Applied Mathematics
Northwestern University, Evanston, Illinois 60201, USA

Kernforschungszentrum Karlsruhe GmbH, Karlsruhe

Kernforschungszentrum Karlsruhe GmbH
Postfach 3640, 7500 Karlsruhe 1

ISSN 0303-4003

Summary

A horizontal layer is heated from below and cooled from above so that the enclosed two-component liquid is solidified in the upper part of the layer. Davis, Müller & Dietsche (1984) examined the case of a single component liquid in which transport occurs via thermal diffusion and convection. In the present case there is the addition effect of thermosoluted convection including the Sorét effect. For reasons of simplicity it is assumed that the solute is completely rejected from the solid phase and the solid-liquid surface free energy is negligible.

We use linear theory to study the stability of the steady temperature and concentration profile in a two-layer system, a liquid and a solid layer.

In the absence of phase change, the Sorét effect gives rise to an oscillatory onset of convection as shown e.g. by Hurle & Jakeman (1971). In the present work Sorét convection with phase change is studied to determine the influence of the thickness of the solid layer, the effect the latent heat of solidification and the initial concentration on the stability of the system and the oscillation frequency of the convection.

As a result of the analysis, it is found that in case of an overstable transition the oscillation frequency increases with increasing initial concentration of the fluid, with increasing thickness of the solid layer, and for increasing values of the latent heat. Moreover, the system is stabilized for increasing values of the latent heat and the initial concentration and destabilized for increasing values of thickness of the solid layer.

If the onset of convection is stationary for the two component system, the system is destabilized by increasing the initial concentration or the thickness of the solid layer.

Bénard-Konvektion in einer zweikomponentigen Flüssigkeit mit teilweisem Ausfrieren

Zusammenfassung

Eine horizontale, zweikomponentige Flüssigkeitsschicht wird von unten beheizt und von oben so weit abgekühlt, daß die Flüssigkeit im oberen Teil ausfriert. Davis, Müller & Dietsche (1984) haben dies für den Fall einer einkomponentigen Flüssigkeit untersucht, in der der Wärmetransport durch Wärmeleitung und Konvektion erfoglt. Im hier behandelten Fall kommt noch der Effekt der thermischen Diffusion einschließlich des Sorét-Effektes hinzu. Der Einfachheit halber wird angenommen, daß der gelöste Stoff vollständig in der flüssigen Phase verbleibt und die freie Energie der flüssig-fest-Grenzschicht vernachlässigbar klein sei.

Um die Stabilität der stationären Temperatur- und Konzentrationsprofile in der festen und flüssigen Schicht zu untersuchen, wird eine lineare Stabilitätsanalyse durchgeführt.

Tritt kein fest-flüssig-Übergang auf, kann aufgrund des Sorét-Effektes die Konvektion oszillatorisch einsetzen (Hurle, Jakeman (1971)). Hier wird der Sorét-Effekt mit Phasenübergang untersucht und dabei der Einfluß der Eisschichtdicke, der Schmelzwärme und der Anfangskonzentration der Flüssigkeitsmischung auf die Stabilität des Systems und die Oszillationsfrequenz bestimmt.

Ergebnis der Analysen ist, daß im Falle des überstabilen Überganges die Oszillationsfrequenz mit zunehmender Anfangskonzentration, Eisschichtdicke und Schmelzwärme ansteigt. Weiterhin wird das System durch höhere Schmelzwärme und Anfangskonzentrationen stabilisiert, während es größere Eisschichtdicken destabilisieren.

Beginnt die Instabilität als stationäre Konvektion, wird das System bei größeren Anfangskonzentrationen und Eisschichtdicken früher instabil.

1. Introduction

Convection can be the dominant mode of heat and mass transport in many processes that involve the solidification or melting of material. This is the case for the freezing of ponds or bays and the storage of thermal energy based on the melting of the storage material. The solidification in molds of liquid metals or alloys and the growth of crystals from melt or aqueous solutions are cases where double-diffusive processes may be present so that there is the need to understand the interaction in multicomponent systems. Although the effect of convective transport in all these processes has been a subject of many experimental and theoretical investigations (see e.g. Foster (1969), Farhadieh and Tankin (1975), Fischer (1981), Saitoh and Hirose (1980, 1982), Hurle & Jakeman (1981), Marshall (1981)) fundamental uncertainties exist in the prediction of the progress and the shape of the freezing or melting front. The growth of crystals from binary solutions is a process where the interaction of adverse temperature and concentration gradients may generate unwanted interfacial instabilities during a unidirectional solidification (Mullins & Sekerka (1964), Coriell et al. (1980), Coriell and Sekerka (1981), Hurle, Jakeman & Wheeler (1983)). These instabilities generally deform the initially planar solid-liquid interface and lead to a cellular pattern of micro-segregation. The interaction of the temperature and concentration field near a progressing solidification front gives rise to the so-called morphological instability (Mullins, Sekerka (1964); Sekerka (1973); Langer (1980)) in which diffusive processes dominate. Weakly nonlinear theories (Wollkind & Segel (1970), Wollkind & Raissi (1974), Sriranganathan et al. (1983), Caroli et al. (1984, 1985)) lead to prediction of hexagonal patterns for the resulting interfacial corrugations.

Interfacial instabilities may also originate from the onset of solutal or thermal convection in the liquid phase if the gradients are parallel to the gravity vector. Stability criteria based on linear analyses for solutal driven convection have been given for various conditions by Hurle, Jakeman & Wheeler (1982, 1983). They also analyse the complex system of interacting morphological instabilities and solutal convection and show that stationary and oscillatory (overstable) perturbations of the temperature, concentration and velocity may occur when the critical conditions are exceeded.

In previous articles Davis, Müller & Dietsche (hereinafter referred to as DMD) and Dietsche, Müller (1985) focus on a single component system in which thermal convection and corrugations of the solidifying/melting interface are strongly coupled. These authors report an experiment showing that interfacial corrugations are two-dimensional when the solidified layer is thin but hexagonal when it is thick. Furthermore, jump behaviour in the liquid-layer thickness at onset of convection is observed. They present a weakly nonlinear convective instability theory which explains these phenomena, and isolates this 'purely thermal' mechanism of the pattern selection.

In this work we extend the theoretical considerations of DMD to a two-component liquid layer. As in DMD, the layer is subject to heating from below and to cooling from above, the boundary temperature at the top is adjusted so that the upper part of the layer is solidified and there is a solid-liquid interface. In addition we take into account mass transport by convection, by concentration and by thermal diffusion, i.e. we deal with thermosolutal Bénard convection including the Sorét effect. However, we neglect the solid-liquid surface free energy i.e. the Gibbs-Thompson effect. This can be argued by the relatively small curvature of the interfacial corrugations and the smallness of the Gibbs-Thompson coefficient. In the absence of phase change the Sorét effect can give rise to an oscillatory mode at the onset of convection (see e.g. Hurle & Jakeman (1971), Caldwell (1970), Platten & Chavepeyer (1973)). Here we study Sorét convection with phase change to determine the effect the latent heat of solidification has on the oscillation frequency. For this we investigate the stability of steady temperature and concentration profile in a partly solidified liquid layer of a constant initial concentration. A linear stability analysis is used.

2. Formulation

Consider the configuration sketched in figure 1 where the horizontal parallel plates of infinite horizontal extent are separated by a distance h. The lower plate at z = 0 is fixed at the temperature $T = T_o$ while the upper plate at z = h is fixed at temperature $T = T_1$. The material between the plates is a two-component liquid if $T > T_s$ and pure solid if $T < T_s$. Thus, the lean component is completely rejected when the liquid solidifies. Gravity of magnitude g is directed downward, the layer is heated from below, $T_1 < T_s < T_o$, and there is a solid-liquid interface at $z = \eta$ with $0 < \eta < h$.

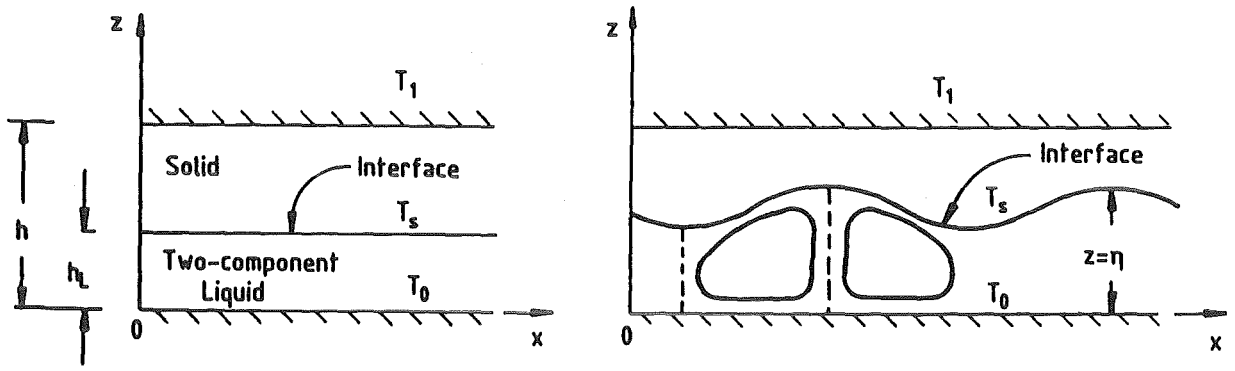

Fig. 1: Schematic drawing of partially solidified liquid layer.

The material properties are the density ρ_o, the specific heat c_p, the thermal conductivity λ, thermometric conductivity $\varkappa$, kinematic viscosity ν, and volume expansion coefficients α and α' for thermal and concentration effects, respectively. The lean component has diffusivity D and Sorét coefficient S_o Superscripts S and L will be used to designate solid and liquid properties when required.

2.1 Boundary Conditions

The coupled effects of buoyancy-driven convection and phase changes will be described by thermal conduction in the solid and the Boussinesq equations

(Mihaljan 1962) in the liquid. At the interface at $z = \eta$, we assume that there is no undercooling due to surface energy (the Gibbs-Thompson effect) so that the temperatures are continuous,

$$T^{(L)} = T^{(S)} = T_s. \tag{2.1}$$

The jump in heat flux is balanced by the production of latent heat L,

$$\rho^{(S)} L \eta_t = [\lambda^{(S)} \nabla T^{(S)} - \lambda^{(L)} \nabla T^{(L)}] \cdot \underset{\sim}{n} N \tag{2.2}$$

where $\underset{\sim}{n}$ is the unit normal vector to the interface

$$\underset{\sim}{n} = (-\eta_x, -\eta_y, 1) N^{-1} , \tag{2.3a}$$

and

$$N = (1 + \eta_x^2 + \eta_y^2)^{1/2} . \tag{2.3b}$$

Subscripts x,y,z,t represent partial differentiation.

The common temperature T_s of the interface, defined in equation (2.1), is unknown a priori since it depends on the concentration $C^{(L)}$ (defined in mole fraction, say) of the lean component at the interface. We write the equilibrium relation, depicting the phase behavior, in a linear form

$$T^{(L)} = T_{so} = T_{sl} + m' C^{(L)} . \tag{2.4}$$

Here m' means the slope of the melting curve of an ideal mixture which is given by

$$m' = -R \cdot T_{sl}^2 / L_l \tag{2.4a}$$

with R being the universal gas constant, L_l the heat of fusion of component 1 and T_{sl} its melting temperature.

The lean component mass balance at the interface takes the form

$$\rho^{(S)} C^{(L)} \eta_t = \rho_o^{(L)} \underset{\sim}{j} \cdot \underset{\sim}{n} N \tag{2.5}$$

since the concentration of the lean component in the solid is zero. Here the

flux $\underset{\sim}{j}$, allowing for Sorét diffusion, takes the form

$$\underset{\sim}{j} = -D[\nabla C^{(L)} + S_o\, C^{(L)}\,(1-C^{(L)})\,\nabla T^{(L)}]\,. \tag{2.6}$$

The interface is non-mobile but deformable so that there is the kinematic condition

$$N\,\rho_o^{(L)}\;\underset{\sim}{v}\cdot\underset{\sim}{n} = (\rho_o^{(L)} - \rho_o^{(S)})\,\eta_t \tag{2.7}$$

and the no slip condition

$$\underset{\sim}{v}\cdot\underset{\sim}{t}^{(1)} = \underset{\sim}{v}\cdot\underset{\sim}{t}^{(2)} = 0 \tag{2.8}$$

where $\underset{\sim}{t}^{(1)}$ and $\underset{\sim}{t}^{(2)}$ are unit tangent vectors

$$\underset{\sim}{t}^{(1)} = (1 + \eta_y^2,\ -\eta_x\,\eta_y,\ \eta_x)(1 + \eta_y^2)^{-1/2}\,N^{-1}, \tag{2.9a}$$

$$\underset{\sim}{t}^{(2)} = (0,\ 1,\ \eta_y)(1 + \eta_y^2)^{-1/2}. \tag{2.9b}$$

At the upper plate at z = h, the temperature is fixed,

$$T^{(S)} = T_1\,. \tag{2.10}$$

At the lower plate at z = 0, the temperature is fixed, the plate is rigid and immobile,

$$T^{(L)} = T_o \tag{2.11a}$$

$$\underset{\sim}{v} = \underset{\sim}{0}\,, \tag{2.11b}$$

$$\underset{\sim}{j}\cdot\underset{\sim}{k} = 0\,. \tag{2.11c}$$

where

$$\underset{\sim}{k} = (0,\ 0,\ 1). \tag{2.12}$$

The equation (2.11b) for the velocity vector $\underset{\sim}{v}$ includes the no slip and impenetrability conditions while equation (2.11c) states the vanishing of the mass flux of the lean component.

2.2 Differential Equations

In the solid, there is only diffusion of heat,

$$T_t^{(S)} = \kappa^{(S)} \nabla^2 T^{(S)} . \tag{2.13}$$

In the liquid, there are the Boussinesq equations (see Coriell & Sekerka 1981),

$$\underset{\sim}{v}_t + \underset{\sim}{v}\cdot\nabla\underset{\sim}{v} = -\frac{1}{\rho_o^{(L)}} \nabla p + \nu\nabla^2 \underset{\sim}{v} + [\alpha(T-T_{so}) + \alpha' C]\, g\, \underset{\sim}{k} , \tag{2.13a}$$

$$\nabla\cdot\underset{\sim}{v} = 0 , \tag{2.13b}$$

$$T_t^{(L)} + \underset{\sim}{v}\cdot\nabla T^{(L)} = \kappa^{(L)} \nabla^2 T^{(L)} , \tag{2.13c}$$

$$C_t^{(L)} + \underset{\sim}{v}\cdot\nabla C^{(L)} = -\nabla\cdot\underset{\sim}{j} , \tag{2.13d}$$

$$\rho = \rho_o^{(L)} \left[1 - \alpha(T - T_{so}) - \alpha' C\right] \tag{2.13e}$$

where we have used a linear equation of state (eq. 2.13e) for the density in the buoyancy term of equation (2.13a) and T_{so} is a reference temperature to be defined shortly.

2.3 Static Equilibrium Solution

In order to define the mass of the lean component we imagine the whole layer to be occupied at time $t = 0$ by a homogeneous two-component liquid with concentration C_o. When the layer is partially solidified, there is the overall mass balance for this component,

$$C_o h = \frac{1}{A} \int_A \int_o^{\eta} C^{(L)} \, dz \, dA \tag{2.14}$$

where A represents the horizontal area of one spatial period in the convection. The z-integration interval reflects the absence of the lean component in the solid.

The governing system possesses a static equilibrium solution in which the interface is planar at $z = \eta = h_L$, the velocity vector $\underset{\sim}{v}$ is identically zero, the pressure p is hydrostatic and the temperatures are purely conductive. Here,

$$\bar{T}^{(L)} = T_{so} - (T_o - T_{so}) \frac{z-h_L}{h_L} \tag{2.15a}$$

and

$$\bar{T}^{(S)} = T_{so} - (T_{so} - T_1) \frac{z-h_L}{h-h_L} \quad . \tag{2.15b}$$

Fields (2.15) satisfy conditions (2.1), (2.10) and (2.11a). The flux condition (2.2) further constrains the parameters so that

$$\frac{h_S}{h_L} = \frac{\lambda^{(S)}}{\lambda^{(L)}} \frac{T_{so}-T_1}{T_o-T_{so}} \equiv B \tag{2.16}$$

where

$$h = h_S + h_L \quad . \tag{2.17}$$

Here T_{so} is the (concentration-dependent) interface temperature T_s in the basic state. To determine the value of T_{so} and hence the temperature gradients, we must find $\bar{C}^{(L)}$. We solve equations (2.13d) and (2.6) subject to condition (2.11c) and find that

$$\bar{C}_z^{(L)} + S_o \bar{C}^{(L)} (1-\bar{C}^{(L)}) \bar{T}_z^{(L)} = 0 \quad . \tag{2.18}$$

This automatically satisfies condition (2.5).

The solution of equation (2.18), given $\bar{T}^{(L)}$ from (2.15a) is

$$\bar{C}^{(L)} = \left\{1 + \frac{1-\bar{C}^{(L)}(h_L)}{\bar{C}^{(L)}(h_L)} \exp\left[-\frac{T_o-T_{so}}{h_L} S_o(z-h_L) \right]\right\}^{-1} \tag{2.19}$$

where the constant of integration, the interface concentration $\bar{C}^{(L)}(h_L)$ is determined through the conservation law (2.14). We obtain from

$$C_o h = \int_o^{h_L} \bar{C}^{(L)} \, dz \tag{2.20}$$

that

$$\bar{C}^{(L)}(h_L) = \frac{\exp\left[-\frac{(T_o-T_{so})}{h_L} S_o h C_o\right] - 1}{\exp\left[-\frac{(T_o-T_{so})}{h_L} S_o h_L\right] - 1} \quad . \tag{2.21}$$

Given $\bar{C}^{(L)}$, we have from equation (2.4) the interface temperature T_{so},

$$T_{so} = T_{s1} + m' \bar{C}^{(L)}(h_L) . \tag{2.22}$$

Thus, the thicknesses of the solid and liquid layers are determined by T_o, T_1, T_{so} and C_o. In particular, as $B \to 0$, the solid disappears.

2.4 Equations in Dimensionless Form

We now introduce the following scales:

$$\begin{aligned} x,y,z &\sim h_L , \\ t &\sim h_L^2/\varkappa^{(L)} , \\ u,v,w &\sim \varkappa^{(L)}/h_L , \\ p &\sim \rho_o^{(L)} \nu \varkappa^{(L)}/h_L^2 , \\ T-T_{so} &\sim T_o - T_{so} , \\ C^{(L)} &\sim C_o . \end{aligned} \tag{2.23}$$

We use the same symbols as before to denote non-dimensional quantities; the full governing Boussinesq system is as follows:

$$P^{-1} [\underset{\sim}{v}_t + \underset{\sim}{v}\cdot\nabla\underset{\sim}{v}] = -\nabla p + \nabla^2 \underset{\sim}{v} + [RT^{(L)} + R_s P S_c^{-1} C_o C^{(L)}] \underset{\sim}{k} , \tag{2.24a}$$

$$\nabla\cdot\underset{\sim}{v} = 0, \tag{2.24b}$$

$$T_t^{(L)} + \underset{\sim}{v}\cdot\nabla T^{(L)} = \nabla^2 T^{(L)} , \tag{2.24c}$$

$$S_c P^{-1} [C_t^{(L)} + \underset{\sim}{v}\cdot\nabla C^{(L)}] = -\nabla\cdot\underset{\sim}{j} , \tag{2.24d}$$

where

$$\underset{\sim}{j} = -[\nabla C^{(L)} + S\, C^{(L)} (1-C_o C^{(L)})\, \nabla T^{(L)}] . \tag{2.24e}$$

Condition (2.14) becomes

$$\frac{h}{h_L} = \frac{1}{A} \int_A \int_o^{\eta} C^{(L)} \, dz \quad . \tag{2.24f}$$

On $z = 0$,

$$T^{(L)} = 1, \tag{2.25a}$$

$$\underset{\sim}{v} = \underset{\sim}{0}, \tag{2.25b}$$

$$\underset{\sim\sim}{jk} = 0. \tag{2.25c}$$

On $z = 1+B$,

$$T^{(S)} = -B/\lambda. \tag{2.26}$$

On $z = \eta$,

$$T^{(S)} = T^{(L)}, \tag{2.27a}$$

$$\rho \, Ste \, \eta_t = [\lambda \nabla T^{(S)} - \nabla T^{(L)}] \cdot \underset{\sim}{n} \, N \quad , \tag{2.27b}$$

$$T^{(L)} = \frac{T_{s1} - T_{so}}{T_{so} - T_o} + m \, C_o \, C^{(L)} \quad , \tag{2.27c}$$

$$S_c P^{-1} \rho C^{(L)} \eta_t = \underset{\sim}{j} \cdot \underset{\sim}{n} \, N, \tag{2.27d}$$

where

$$(1 - \rho) \, \eta_t = \underset{\sim}{v} \cdot \underset{\sim}{n} \, N \quad , \tag{2.27e}$$

$$\underset{\sim}{v} \cdot \underset{\sim}{t}^{(1)} = \underset{\sim}{v} \cdot \underset{\sim}{t}^{(2)} = 0 \, . \tag{2.27f}$$

In the above system there are the following non-dimensional numbers:

$$R = \frac{\alpha g \, (T_o - T_{so}) \, h_L^3}{\varkappa^{(L)} \nu} \quad , \tag{2.28a}$$

$$R_s = \frac{\alpha' \, g \, h_L^3}{D \nu} \quad , \tag{2.28b}$$

$$\mathcal{B} = \frac{\lambda^{(S)}}{\lambda^{(L)}} \frac{T_{so}-T_1}{T_o-T_{so}} \quad , \tag{2.28c}$$

$$P = \frac{\nu}{\varkappa^{(L)}} \quad , \tag{2.28d}$$

$$S_c = \frac{\nu}{D} \quad , \tag{2.28e}$$

$$\rho = \frac{\rho_o^{(S)}}{\rho_o^{(L)}} \quad , \tag{2.28f}$$

$$\lambda = \frac{\lambda^{(S)}}{\lambda^{(L)}} \quad , \tag{2.28g}$$

$$\varkappa = \frac{\varkappa^{(S)}}{\varkappa^{(L)}} \quad , \tag{2.28h}$$

$$Ste = \frac{\rho_o^{(L)} \, L \, \varkappa^{(L)}}{\lambda^{(L)} (T_o-T_{so})} \quad , \tag{2.28i}$$

$$S = S_o \, (T_o-T_{so}) \quad , \tag{2.28j}$$

$$m = \frac{m'}{T_o-T_{so}} \quad , \tag{2.28k}$$

$$c_o \quad . \tag{2.28l}$$

System (2.24) - (2.28) governs the full nonlinear coupled solidification/convection problem. The basic state (2.15) - (2.22) can now be written in non-dimensional terms as follows:

$$\bar{T}^{(L)} = 1 - z, \tag{2.29a}$$

$$\bar{T}^{(S)} = \lambda^{-1}(1 - z), \tag{2.29b}$$

$$\frac{h}{h_L} - 1 = \frac{h_S}{h_L} = \lambda \frac{T_{so} - T_1}{T_o - T_{so}} \equiv \mathcal{B} , \tag{2.29c}$$

$$\bar{C}^{(L)} = \{C_o + \frac{1 - C_o \bar{C}^{(L)}(1)}{\bar{C}^{(L)}(1)} \exp [S(1 - z)]\}^{-1} , \tag{2.29d}$$

where

$$\bar{C}^{(L)}(1) = \frac{\exp [-(1+\mathcal{B}) S C_o] - 1}{\exp [- S] - 1} \frac{1}{C_o} \tag{2.29e}$$

Given the value of $\bar{C}^{(L)}(1)$, equation (2.22) determines the (dimensional) interface temperature T_{so} used in the scaling.

3. Linear Stability Theory

We perturb the governing system about the static basic state (2.29) and obtain the following linear stability equations:

$$P^{-1}\underset{\sim}{v}'_t = -\nabla p' + \nabla^2 \underset{\sim}{v}' + [RT' + R_s P S_c^{-1} C_o C'] \underset{\sim}{k} \quad , \tag{3.1a}$$

$$\nabla \cdot \underset{\sim}{v}' = 0 \quad , \tag{3.1b}$$

$$T'_t = \nabla^2 T' + \underset{\sim}{v}' \cdot \underset{\sim}{k} \quad , \tag{3.1c}$$

$$S_c P^{-1} C'_t = -\nabla \cdot \underset{\sim}{j}' - S_c P^{-1} \bar{C}_z^{(L)} \underset{\sim}{v}' \cdot \underset{\sim}{k} \tag{3.1d}$$

where

$$\underset{\sim}{j}' = -\{\nabla C' + S[\bar{C}^{(L)}(1-C_o\bar{C}^{(L)})\cdot\nabla T' - (1-2C_o\bar{C}^{(L)})C'\underset{\sim}{k}]\} \quad , \tag{3.1e}$$

$$T_t^{(S)} = \varkappa \nabla^2 T^{(S)} \quad . \tag{3.2}$$

On $z = 0$,

$$T' = 0 \tag{3.3a}$$

$$\underset{\sim}{v}' = \underset{\sim}{0} \tag{3.3b}$$

$$\underset{\sim}{j}' \cdot \underset{\sim}{k} = 0 \tag{3.3c}$$

On $z = 1 + B$,

$$T' = 0 \quad . \tag{3.4}$$

On $z = 1$,

$$T^{(S)'} - T' = -\eta(1 - \lambda^{-1}) \quad , \tag{3.5a}$$

$$\rho \, \mathrm{Ste} \, \eta_t = \lambda T_z^{(S)'} - T'_z \quad , \tag{3.5b}$$

$$T' - \eta = m C_o (C' + \eta \bar{C}_z^{(L)}(1)) \quad , \tag{3.5c}$$

$$S_c P^{-1} \rho \bar{C}^{(L)} \eta_t = \underset{\sim}{j}' \cdot \underset{\sim}{k} \quad , \tag{3.5d}$$

$$(1 - \rho)\, \eta_t = \underset{\sim}{v'} \cdot \underset{\sim}{k} \quad , \tag{3.5e}$$

$$\underset{\sim}{v'} \times \underset{\sim}{k} = \underset{\sim}{0} \tag{3.5f}$$

where we have used forms (2.29a,b). For spatially periodic disturbances, condition (2.24f) is automatically satisfied. We have omitted the superscript "L" on the fields in the liquid and primes to denote perturbation quantities.

We introduce normal modes for each disturbance quantity ϕ' as follows:

$$\Phi'(x,y,z,t) = \Phi e^{-\omega t + i(k_1 x + k_2 y)} \tag{3.6a}$$

where

$$k = (k_1^2 + k_2^2)^{1/2} \tag{3.6b}$$

and introduce the velocity components

$$\underset{\sim}{v'} = (u', v', w') \tag{3.7}$$

and we denote d/dz by D.
We eliminate u', v', p' from equations (3.1a,b) by cross differentiation to obtain:

$$(D^2 - k^2)(D^2 - k^2 + \omega P^{-1})\, W - k^2 [RT + R_s P S_c^{-1} C_o C] = 0 . \tag{3.8a}$$

Forms (3.1c,d) becomes

$$(D^2 - k^2 + \omega)\, T + W = 0, \tag{3.8b}$$

$$-DJ_3 - k^2 [C + S \bar{C}^{(L)} (1 - C_o \bar{C}^{(L)}) T] + \omega S_c P^{-1} C - S_c P^{-1} \bar{C}_z^{(L)} W = 0 , \tag{3.8c}$$

where

$$-J_3 = DC + S[\bar{C}^{(L)} (1 - C_o \bar{C}^{(L)})\, DT - (1 - 2C_o \bar{C}^{(L)})\, C] . \tag{3.8d}$$

In the solid, equation (3.2) gives

$$(D^2 - k^2 + \omega \varkappa^{-1}) T^{(S)} = 0 . \tag{3.9}$$

On $z = 0$,
$$T = W = DW = J_3 = 0 \ . \tag{3.10}$$
On $z = 1+B$,
$$T = 0 \ . \tag{3.11}$$
On $z = 1$,

$$T^{(S)} - T = -H\,(1 - \lambda^{-1}) \ , \tag{3.12a}$$

$$-\omega\rho\,\mathrm{Ste}\,H = \lambda\,DT^{(S)} - DT \ , \tag{3.12b}$$

$$T - H = mC_o\,[C + H\,\bar{C}_z^{(L)}\,(1)] \ , \tag{3.12c}$$

$$-\omega\rho\,S_c P^{-1}\,\bar{C}^{(L)}\,H = \underset{\sim}{j}\cdot\underset{\sim}{k} = J_3 \tag{3.12d}$$

$$-\omega\,(1-\rho)\,H = W \ , \tag{3.12e}$$

$$DW = 0 \ . \tag{3.12f}$$

We solve equation (3.9) subject to the conditions (3.11) and (3.12) we obtain:

$$T^{(S)}{}_{(z)} = [T + (\lambda^{-1} - 1)H\,]\,\tilde{\Lambda}\,(\zeta) \tag{3.13a}$$

where

$$\zeta = \frac{z-1}{\mathcal{B}} \ , \tag{3.13b}$$

$$\tilde{\Lambda} = \frac{\sinh\delta\mathcal{B}(1-\zeta)}{\sinh\delta\mathcal{B}} \ , \tag{3.13c}$$

and
$$\delta = (k^2 - \omega\varkappa^{-1})^{1/2} \ . \tag{3.13d}$$

We now evaluate condition (3.12b), using forms (3.13), and eliminating H by using condition (3.12c). We obtain:

$$\begin{aligned} &DT + \{\mathcal{L}\,[1 + \lambda m C_o\,\bar{C}_z^{(L)}(1)] - \omega\rho\,\mathrm{Ste}\}\,\{1 + m\,C_o\bar{C}_z^{(L)}(1)\}^{-1}\,T \\ &\quad - mC_o[\mathcal{L}(1-\lambda) - \omega\rho\,\mathrm{Ste}]\,\{1 + mC_o\,\bar{C}_z^{(L)}\,(1)\}^{-1}\,C = 0 \ . \end{aligned} \tag{3.14a}$$

where

$$\mathcal{L} = -\mathcal{B}^{-1} \left.\frac{d}{d\xi} \tilde{\Lambda} \ (\zeta)\right|_{\zeta=0} = \delta \coth \delta\mathcal{B} . \tag{3.14b}$$

Condition (3.12d), using equation (3.12c) becomes

$$J_3 = -\omega \rho S_c P^{-1} \ \overline{C}^{(L)} \ [T - mC_o C][1 + mC_o \overline{C}^{(L)} \ ]^{-1}, \tag{3.14c}$$

Condition (3.12e) using equation (3.12c) becomes

$$W + \omega(1 - \rho) \ [T - mC_o C] \ [1 + mC_o \ \overline{C}_z^{(L)} \ ]^{-1} = 0, \tag{3.14d}$$

while conditions (3.12f) remains

$$DW = 0 . \tag{3.14e}$$

The result of the linear stability analysis is a system of differential equations for the z-dependent perturbance quantities in the fluid (eq. 3.8) and expressions for the corresponding boundary conditions at z = 0 (eq. 3.10) and z = η (eq. 3.14).

4. Numerical Evaluation of the Eigenvalue Problem for the Liquid Layer

The numerical evaluation of the problem is aimed at determining the critical Rayleigh-number R_c and the critical wave number k_c as a function of the various properties and dynamical groups. We consider the two possibilities; the eigenvalues ω are real or the eigenvalues are complex. This means physically that the principle of exchange of stabilities holds or that the instability sets in as an oscillatory convection, i.e. as an overstability. Since in either case we seek only the marginal state, we have to determine either the set $(R_s^{(s)}, k_c^{(s)})$ or the set $(R_c^{(p)}, k_c^{(p)})$, where $\omega^{(p)}$ is the imaginary part of the complex frequency ω. Here the superscripts "s" and "p" denote steady or periodic onset of convection.

The numerical procedure for both cases is the same. The complex higher order system (eqs. 3.8a-d) together with the corresponding boundary conditions (eqs. 3.10, 3.15) is transformed to a real system of sixteen ordinary differential equations for the unknown variables, the real and imaginary parts of W, C, T and their higher derivatives.

For solving the boundary-eigenvalue problem the SUPORE CODE of Scott and Watts (1979) is used. The code is based on a shooting method utilizing orthonormalization of the independent solutions to eliminate linear dependencies between different numerical generated solutions.

The actual solving procedure is as follows: First, assuming that the principle of exchange of stabilities holds, i.e. $\omega = 0$, start values for the wave number k and the Rayleigh number R are chosen as input data for the code. The subroutine SUPORE then calculates the true eigenvalue R* for the given k. Then k is varied and the calculations are repeated until the minimum value R_c is obtained for the particular k_c. The two values form the sought-after set $(R_c^{(s)}, k_c^{(s)})$.

Assuming that the instability sets in as an overstable convection i.e. that is a complex number, we start the computations with a set of input parameters k, R and $\mathrm{Im}(\omega) = \omega_I$. Since we are only interested in the eigenvalues of the marginal state, the real part of ω is taken zero. As a result of the computations we obtain a complex value R for given values of ω_I and k.

Next ω_I is varied until the imaginary part of R vanishes. This is followed by an iteration procedure on k until R* attains its minimum value. As a result of this variational procedure we obtain the sought-after set of eigenvalues $(R_c(p);\ k_c(p), \omega_c(p))$.

The physical properties of the fluid which are kept fixed are characterized by the three groups, the Prandtl number, set as P = 10, the Smidt number, set as $S_c = 10^3$ and the solute Rayleigh number, set as $R_s = 1.5 \times 10^7$. These values are typical for organic mixtures.

The effect of the free solid-liquid interface is determined by the property ratios, $\varkappa^{-1} = \lambda = \varrho = 1.001$, the Stefan number, set as Ste = 3.45 and the slope of the melting curve set as m = -100. The thickness of the solidified layer and as a measure for it the Biot number is varied by reducing the temperature T_1 at the upper boundary of the layer. We vary, however, the initial mixture ratio of the two liquids C_o and the Sorét number S. In some screening calculations the Stefan number and the slope m are also varied in order to investigate the effect of the latent heat on the flow oscillations and its critical quantities.

5. Numerical results

a. The effect of diffusion and conduction

It is usual in the literature for the Soret number S to measure the concentration of the richer component which here is liquid 1. In order to have notation compatible with previous work we take $S \equiv S_1 = -S_2$.

We first examine the pure Soret convection problem in which the layer is all liquid and no solidified material is present; here B = 0. Fig. 2 shows for $C_o = 0.01$, the critical Rayleigh number, wave number and oscillation frequency as functions of S.

When S = 0, there is no Soret effect and instability sets in as steady Bénard convection with $R_c^{(s)} = 1709$, $k_c^{(s)} = 3.117$ and $\omega_c = 0$. When S > 0, the instability is still steady, $\omega_c = 0$, and both $R_c^{(s)}$ and $k_c^{(s)}$ decrease with S, consistant with the results of Chock and Li (1975). When S > 0, the Soret diffusion moves the more dense component toward the cold boundary reinforcing the adverse density gradient. When S < 0, the opposite is the case and the stationary instability is opposed, as shown in Fig. 2 and in the results of Chock and Li (1975). In addition, when S is sufficiently negative, $S < S^* < 0$, a new mode, periodic in time, occurs. The corresponding critical Rayleigh number $R_c^{(p)}$ is smaller than $R_c^{(s)}$ for each S. The $k_c^{(p)}$ is slightly smaller than $k_c^{(s)}$ while the frequency ω_c of this oscillatory mode decreases with S and $\omega_c \rightarrow 0$ as $S \rightarrow S^*$. Thus, the modes merge as $S \rightarrow S^*$. Platten and Legros (1984) discuss how S* depends on P, Sc and Rs. The appearance of the oscillatory mode is the result of a double-diffusive mechanism in which the temperature and concentration distributions oppose each other and where their fields diffuse with wastly different time scales, τ_T and τ_c, respectively. Since $\tau_T \ll \tau_c$, a warm fluid element that rises in the layer looses its temperature anomaly in time τ_T which its concentration anomaly remains. The parcel thus is too heavy for its environment, and falls into a warmer layer. If this slower process is on a time scale τ_c, the density of the parcel adjusts to its surroundings, the parcel becomes lighter and rises again due to thermal buoyancy. The cycle thus begins anew.

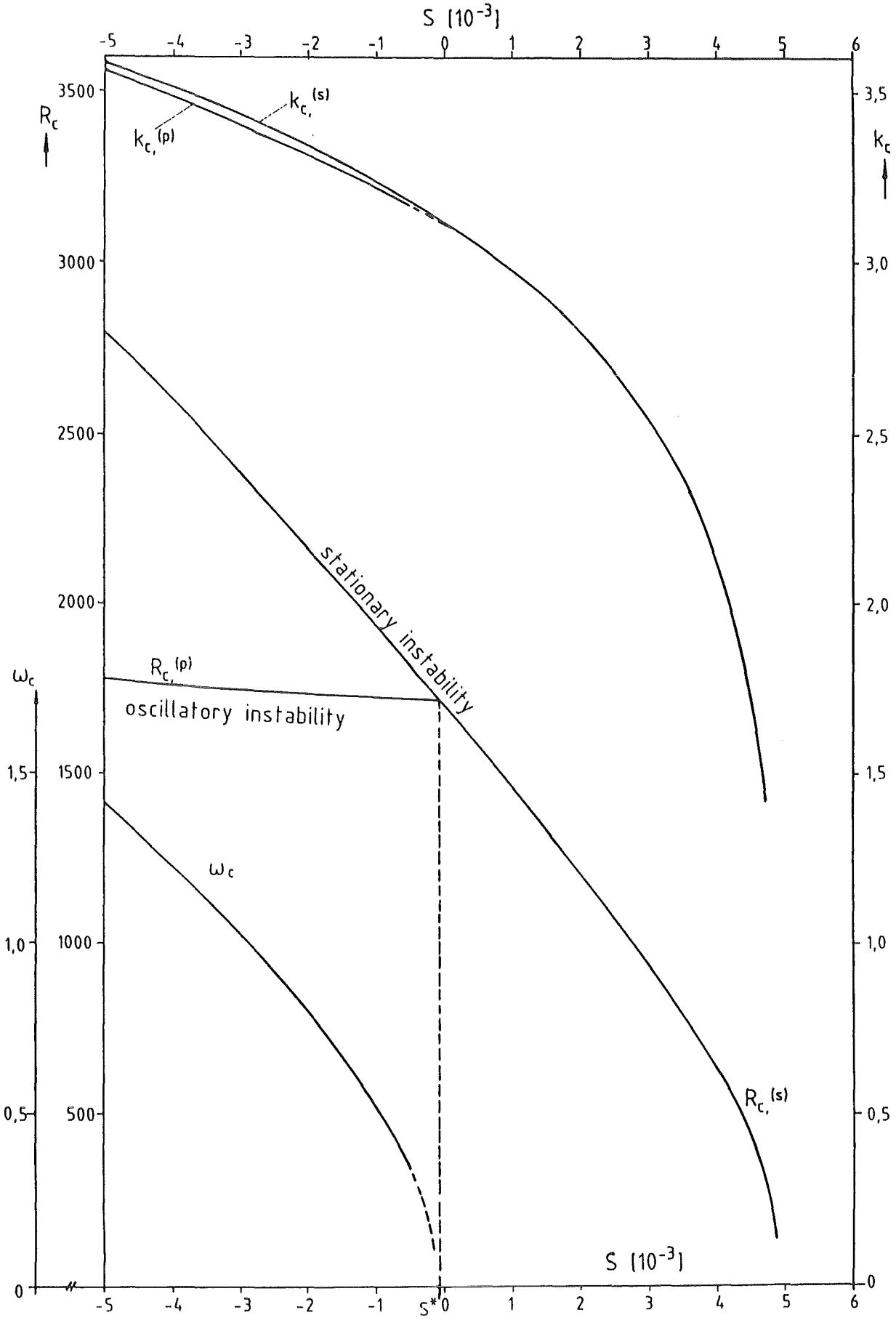

Fig. 2 Critical Rayleigh-number R_c, critical wave number k_c, critical oscillation frequency ω_c as a function of the Sorét-number for an initial concentration $C_o = 0.01$ and a Biot-number $B = 0$. S* denotes the Bifurcation point between steady and oscillatory convection.

b. The effect of initial concentration

We again examine the pure Soret convection problem in the absence of solidified material; here B = 0. Figs. 3-5 show how R_c, k_c and ω_c depend on C_o.

Fig. 3 shows the critical conditions for the stationary instability (which has $\omega_c = 0$). All curves cross at S = 0 where Soret diffusion is absent. $R_c^{(s)}$ decreases with C_o for fixed $S > 0$ as expected since more of the lean component is present to participate in Soret diffusion. Again, as expected, $k_c^{(s)}$ decreases with C_o for fixed $S > 0$.

Fig. 4 shows the critical conditions for the oscillatory instability, which occurs only for $S < S^* < 0$. For fixed S, $R_c^{(p)}$, $k_c^{(p)}$ and ω_c all increase with C_o. Both $R_c^{(p)}$ and $k_c^{(p)}$ increase nearly linearly for $C_o > 0.02$. $R_c^{(p)}$, $k_c^{(p)}$ and ω_c all increase with $|S|$.
The above results are consistant with the idea that an increase in C_o effectively increases S. As can be seen from equs. (3.8 c,d), the Soret diffusion enters the governing equations through a term of the form $S\bar{C}^{(L)}(1 - C_o \bar{C}^{(L)})$. The numerical calculations show for B = 0 that $\bar{C}^{(L)}$ is nearly linear with $|d\bar{C}^{(L)}/dz| < 10^{-3}$. Thus, $\bar{C}^{(L)} \approx C_o$ and if $C_o^2 \ll 1$, then

$$S\,\bar{C}^{(L)}(1-C_o\bar{C}^{(L)}) \approx S\,C_o = S_{eff}. \qquad (5.1)$$

An increase of C_o is equivalent to an increase in $|S|$, consistent with the results of Fig. 4. Note that equ. (3.8 d) has a second term dependent upon S. Given the above argument, it becomes independent of C_o.

Fig. 5 shows the full critical behavior by combining the results of Figs. 3 and 4. Here R_c, k_c and ω_c are shown as functions of S for $C_o = 0.01$ and $C = 0.02$.

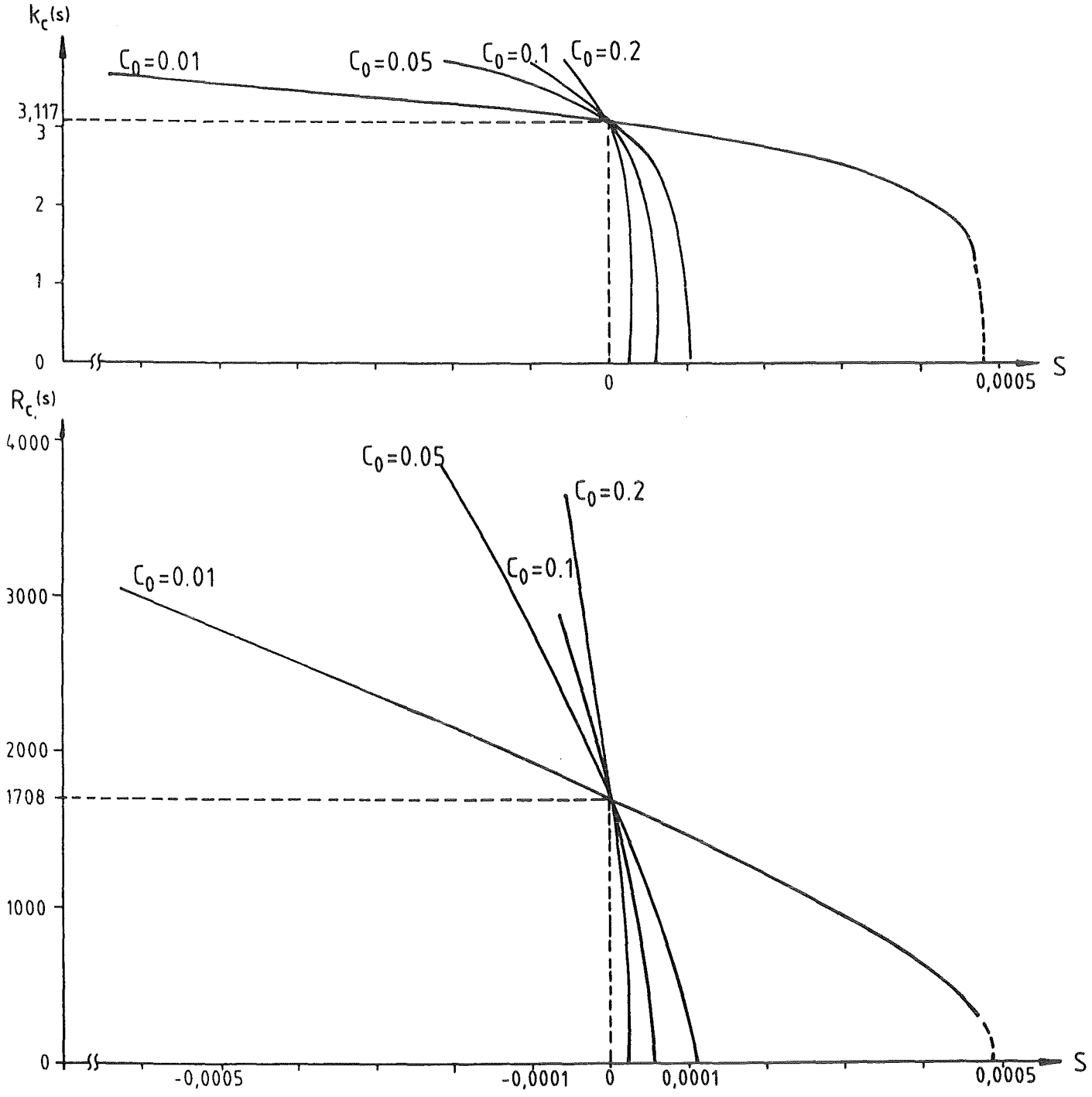

Fig. 3 Critical Rayleigh-number $R_c^{(s)}$ and critical wave number $k_c^{(s)}$ for onset of steady convection as a function of the Soréet-number S and for different initial concentrations C_o = 0.01, 0.05, 0.1, 0.2 and B = 0.

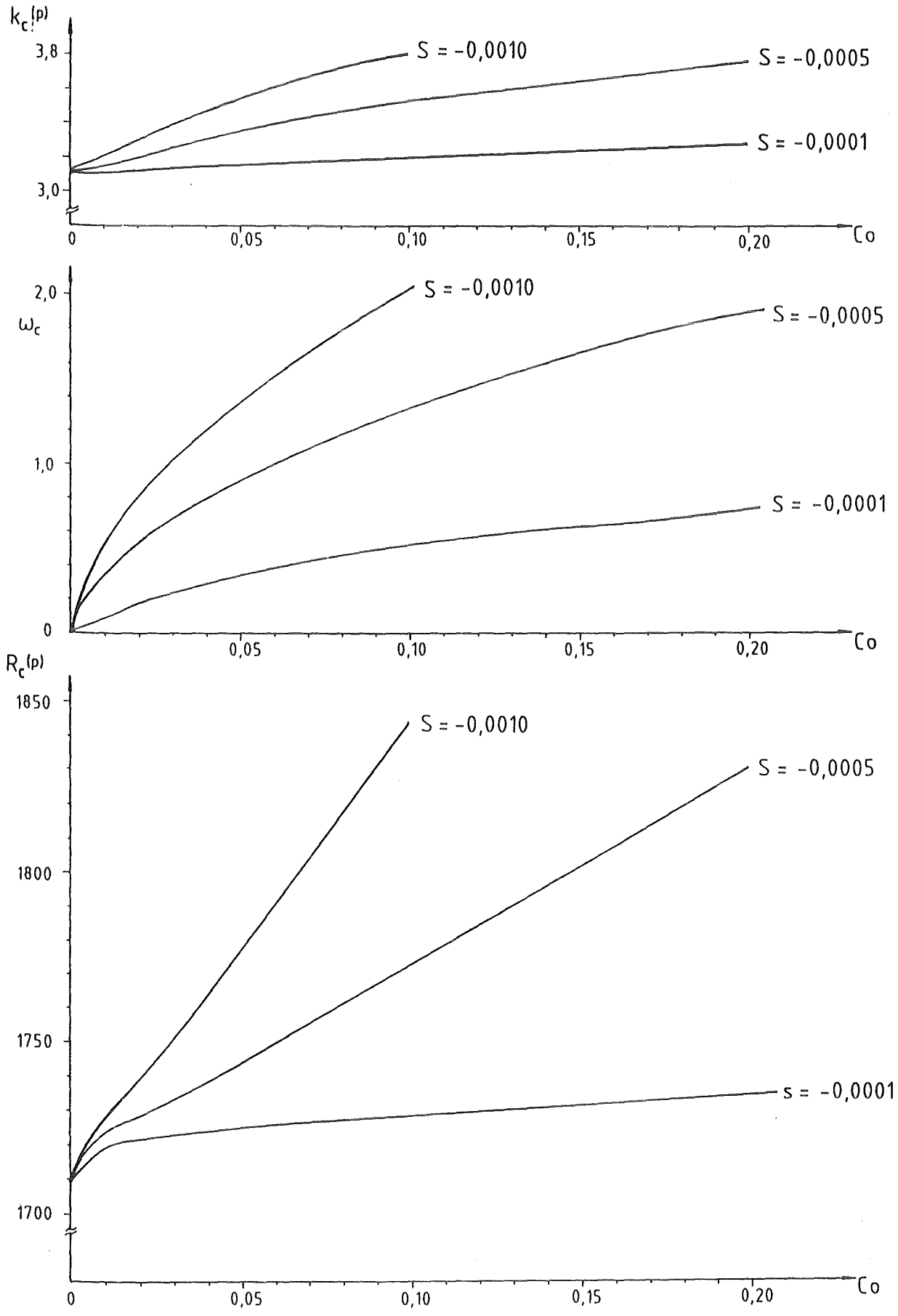

Fig. 4 Critical Rayleigh-number $R_c^{(s)}$, wave number $k_c^{(p)}$, frequency ω_c for the onset of oscillatory convection as a function of the initial concentration C_o for different negative Sorét-numbers and for a Biot-number B = 0.

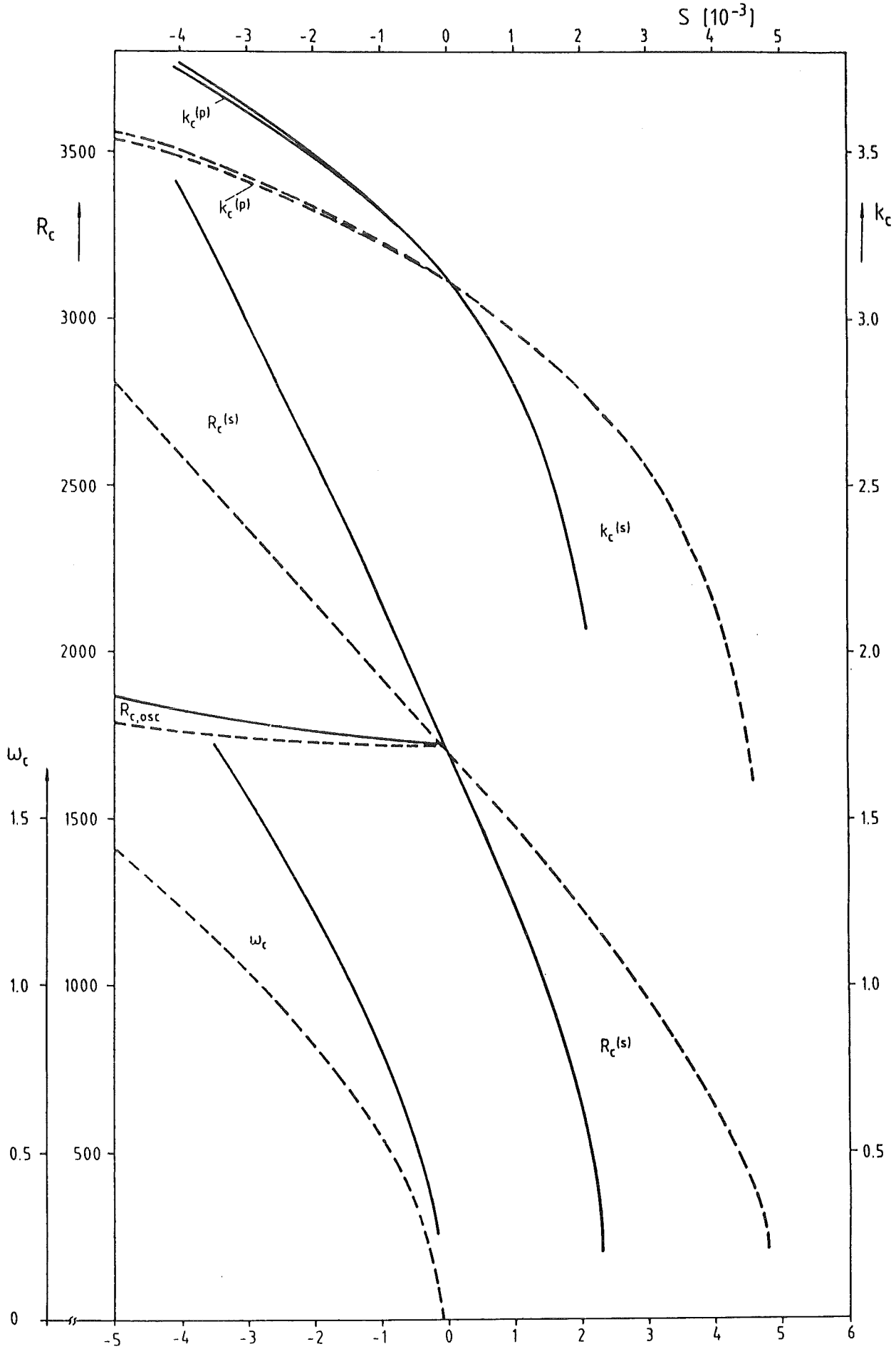

Fig. 5 Critical Rayleigh-number R_c, wave number k_c and oscillation frequency ω_c as a function of the Sorét-number for the initial concentration C_o = 0.01 (dashed line) and C_o = 0.02 (solid line) and B = 0.

c. The effect of the solidified layer

When the layer is partially solidified, $B > 0$ and all of the lean component has been rejected into the liquid. The magnitude of B measures the thickness of the solidified layer. Figs. 6-8 give the critical conditions for $C_o = 0.01$, which is typical for values of C_o not too large, say $C_o < 0.20$.

Fig. 6 shows the critical conditions for instability for the cases $B = 0$ (reproduced from Fig. 2) and $B = 1$. When $S = 0$, Soret diffusion is absent; there is thermal conduction in the solid and conduction and convection in the liquid. This case was treated by Davis, Müller and Dietsche (1984). They find that the presence of the solidified layer affects the thermal environment seen by the thermal perturbations in the liquid. When $B = 0$, the upper boundary of the liquid is a perfect conductor and as B increases, the heat transfer properties of this upper boundary deteriorate. Thus, the thicker the solid layer the lower the R_c for the onset of convection. This is seen in Fig. 6 for $S = 0$; $R_c^{(s)}(B = 1) < R_c^{(s)}$ $(B = 0)$. We saw earlier that in the absence of a solidified layer, that $R_c^{(s)}$ decreases with S. Thus, the two mechanisms reinforce each other. We do see that by making $S < 0$ and greater in magnitude that the Soret effect stabilizes and hence there is a cross-over point ($S \approx -1.5 \times 10^{-3}$, $B = 1.0$) where the two effects balance and $R_c^{(s)}$ has the same value as for $B = 0$. This balancing can be seen in Figs. 7 and 8. For $S < 0$, the curves of $R_c^{(s)}$ versus B have minima indicated by the arrows. For $S > 0$, $R_c^{(s)}$ decreases monotonically with $R_c^{(s)}$ approaching the limiting value obtained by DMD when $S \to 0$.

The above behavior derives from the property that the solid rejects all of the lean component so that for a given C_o its actual concentration in the liquid is greater the thicker the solid layer. Given the approximation above for $\bar{C}^{(L)}$, eq. (2.29e) implies that $\bar{C}^{(L)} \approx (1+B)C_o$ so that now

$$S_{eff} \approx SC_o \cdot (1+B). \tag{5.2}$$

Thus, if $B = 1$, we have effectively doubled C_o or equivalently S. Fig. 8 shows that for $S < 0$ $R_c^{(p)}$ and $k_c^{(p)}$ are quite insensitive to changes in B though ω_c increases monotonically with B and $|S|$. This variation is particularly strong for $B < 0.30$ and $S < -5 \times 10^{-4}$. This is due to the fact that ω_c changes with S more rapidly near $S = S^*$ than elsewhere.

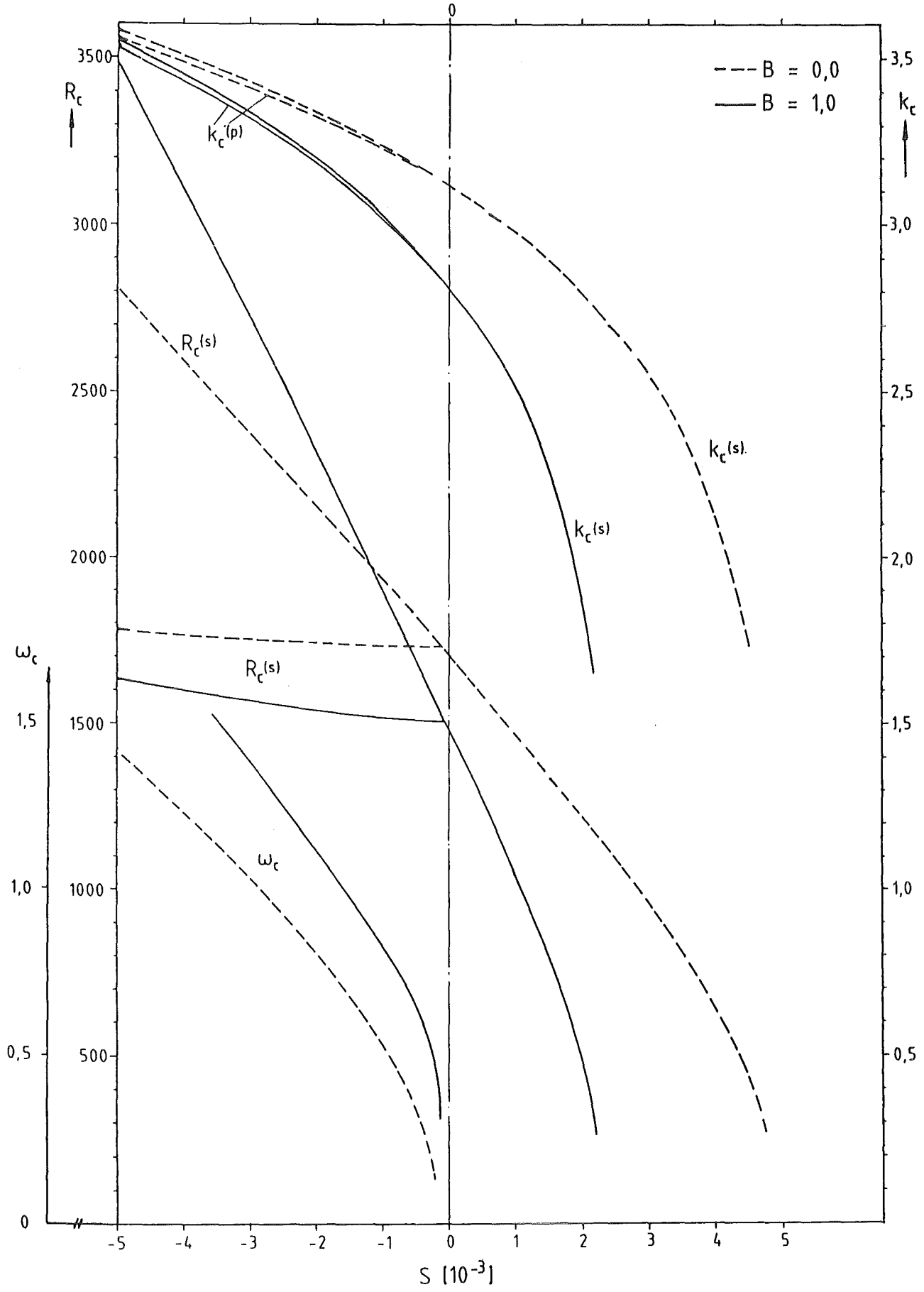

Fig. 6 Critical Rayleigh-numbers, wave numbers k_c and oscillation frequencies ω_c as a function of the Sorét-number S for the initial concentrations C_o = 0.01 and the Biot-numbers B = 0 (dashed line), B = 1.0 (solid line).

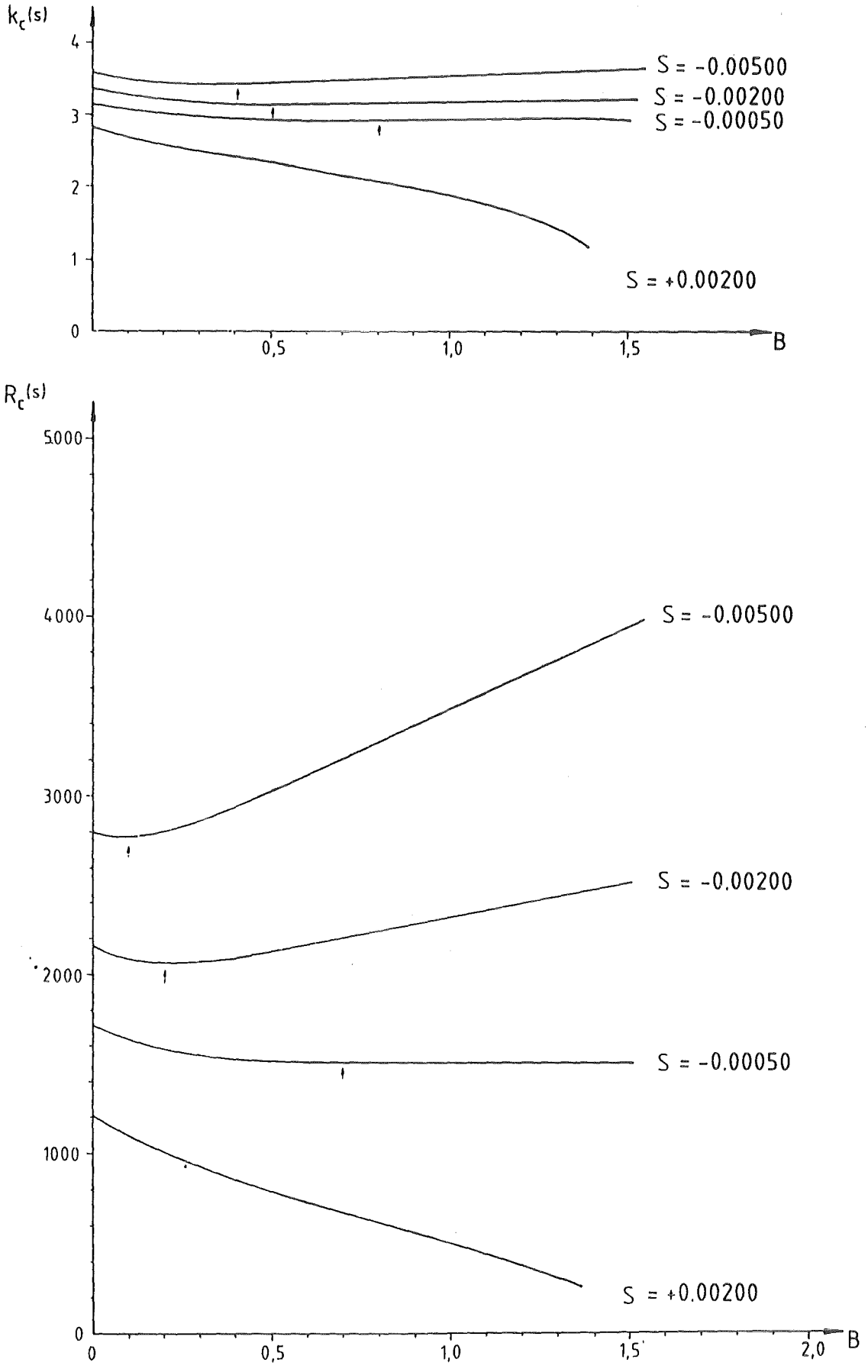

Fig. 7 Critical Rayleigh-numbers $R_c^{(s)}$, wave numbers $k_c^{(p)}$ for the onset of steady convection as a function of the Biot-number for the Sorét-numbers S = +0.0020, -0.0005, -0.0020, -0.0050 and C_o = 0.01.

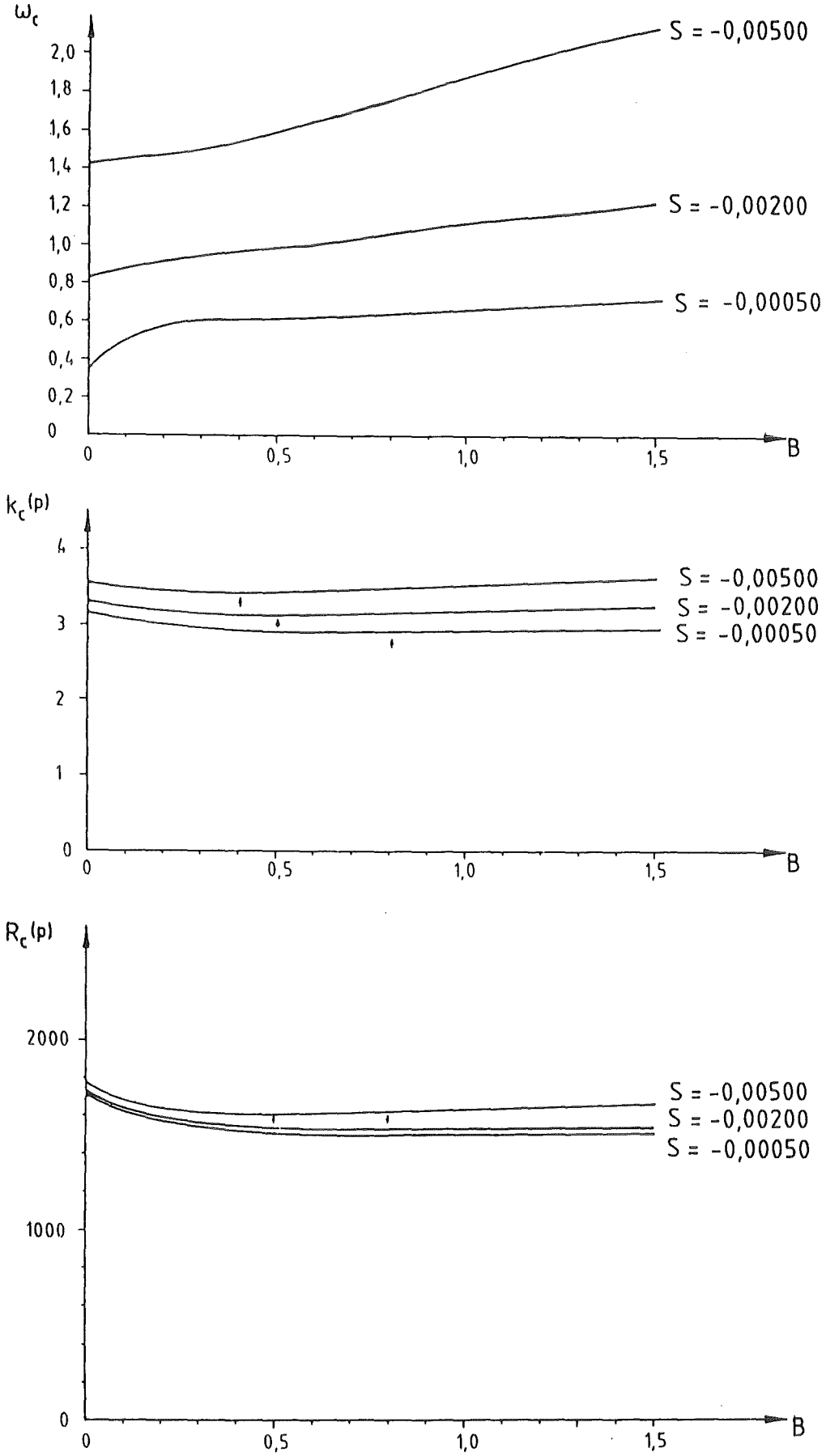

Fig. 8 Critical Rayleigh-number $R_c^{(p)}$, wave number $k_c^{(p)}$ and oscillation frequency ω_c for the onset of oscillatory convection as a function of the Biot-number for different negative Sorét-numbers S = -0.0005, -0.0020, -0.0050 and for the initial concentration C_o = 0.01.

d. The combined effects of the solidifed layer and the initial concentration

Fig. 9 shows $R_c^{(s)}$ versus B for various C_o and S. When S = 0, the value of C_o is immaterial and the value of $R_c^{(s)}$ is that given by DMD. When S < 0 an increase in C_o stabilizes the basic state which is further enhanced by the increase in B. When S > 0, the basic state is destabilized by the increase of either C_o or B.

e. The effect of the latent heat

The latent heat effects the system in two ways. It effects directly through the rate of solidification or melting via the Stefan condition (2.2). It effects the system indirectly through its influence on m, because m varies inversely proportionally to L (equ. (2.4b)) by modifying the melting temperature of the solid.

The present numerical investigation is limited to the case, where the standard value of the latent heat used in the other calculations has been doubled from L = 31.3 kJ/kg to L = 62.6 kJ/kg. The calculations show that the marginal curves of $R_c^{(s)}$ and $k_c^{(s)}$ are practically unchanged by this modification of L; the overall variations are less than 0.1 %. This slight variation is merely due to the effect, that the latent heat modifies the actual melting temperature T_{so} by changing m. This variation of T_{so} is very small (< 1 %) for the considered ranges of C_o and B.

Figs. 10 and 11 show the effect of an enhanced latent heat on the marginal curves $R_c^{(p)}$, $k_c^{(p)}$ and ω_c. The calculations have been performed for a range of B and C_o and for two values of the Sorét number S = - 0.0005 and S = - 005. The graphs show, that $R_c^{(p)}$ is only slightly increased and $k_c^{(p)}$ slightly decreased when the latent heat is doubled (see Figs. 10b and 10c). However, a significant increase of the oscillation frequency ω_c is observed. This effect is particularly strong for negative values of S with small |S|; it vanishes for increasing negative S. It depends moreover on B and C_o (Figs. 10a and 11a).

For the frequency increase of the oscillatory convection in liquids with higher heat of fusion the following explanation is suggested.

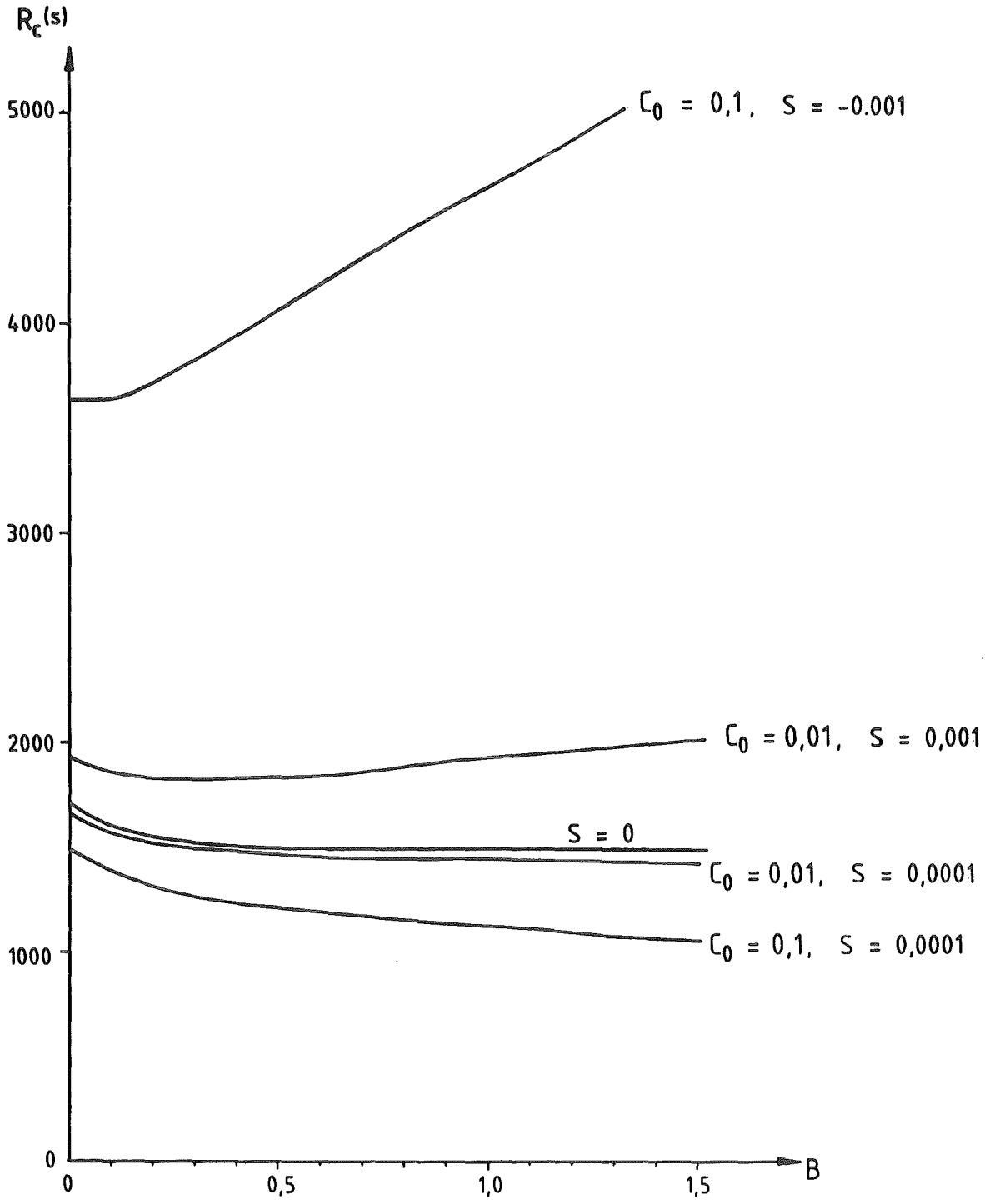

Fig. 9 Critical Rayleigh-number $R_c^{(s)}$ for the onset of steady convection as a function of the Biot-number B for $S > 0$, $S = 0$ and $S < 0$ for the initial concentrations $C_o = 0.01$ and $C_o = 0.1$.

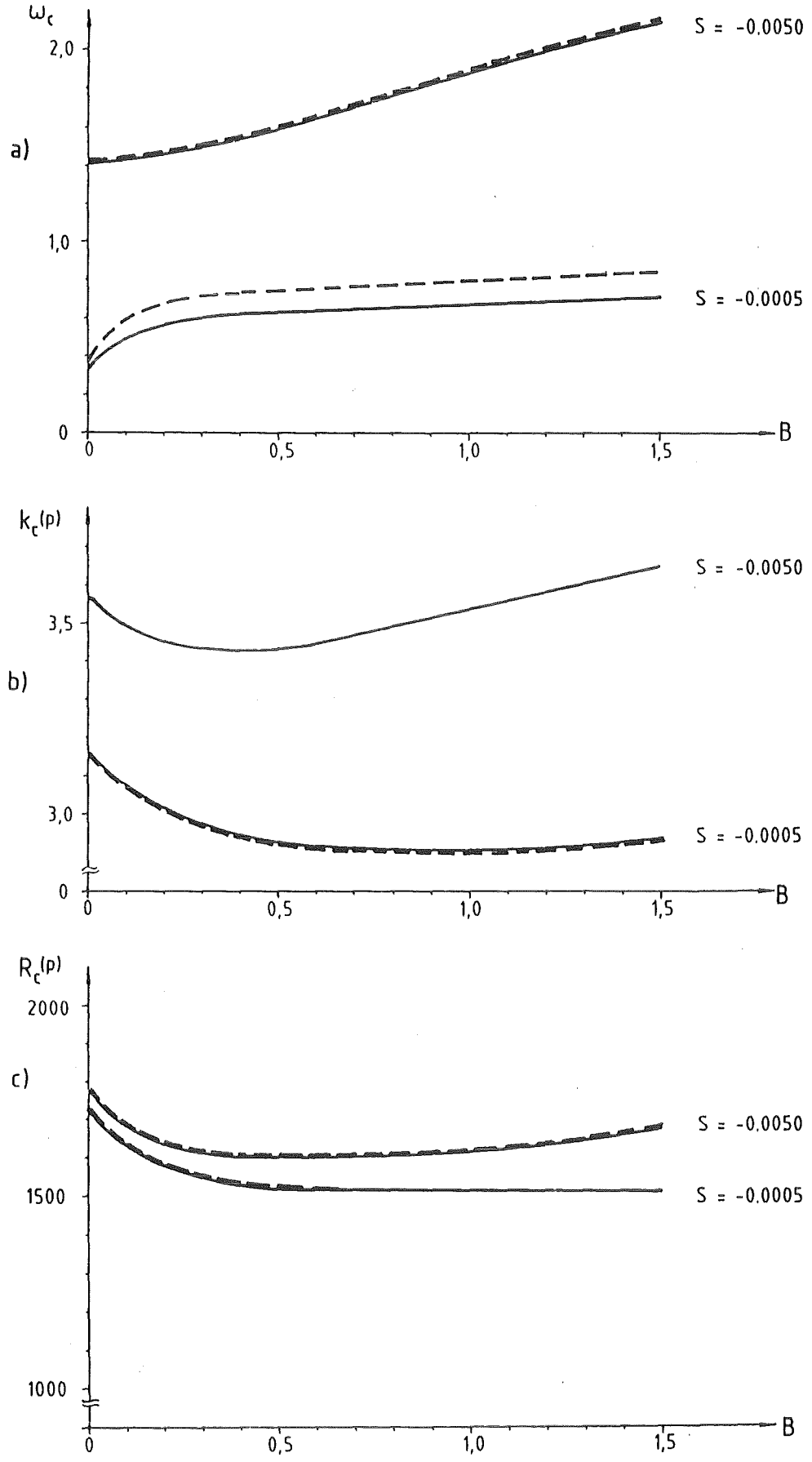

Fig. 10 Critical Rayleigh-numbers $R_c^{(p)}$, wave numbers $k_c^{(p)}$ and frequencies ω_c for the onset of oscillatory convection as a function of the Biot-number B for the initial concentration C_o = 0.01 the Sorét-numbers S = -0.0005, -0.005 and for two values of the latent heat namely L = 31,3 kJ/kg (solid lines) and 2L (dashed lines).

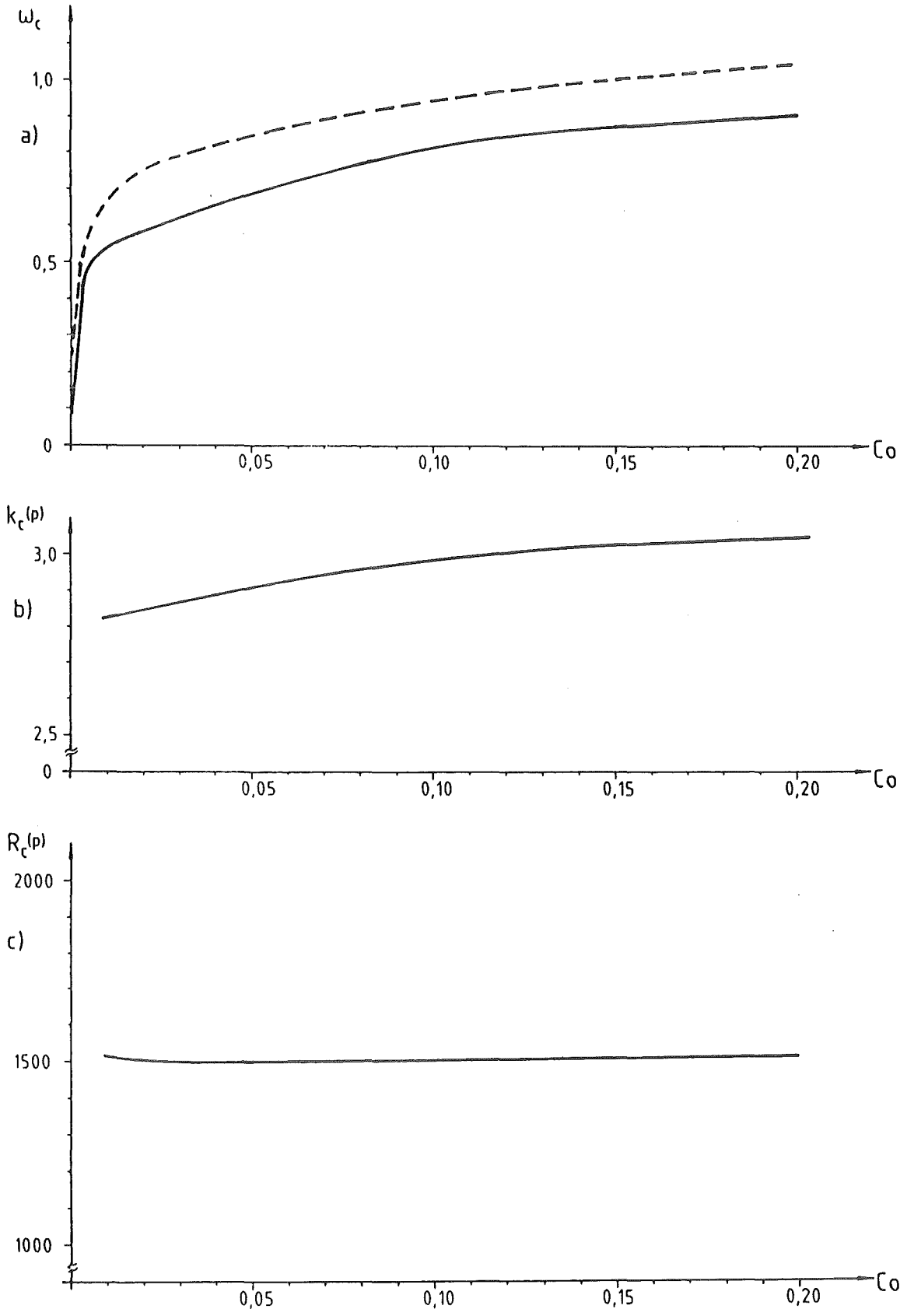

Fig. 11 The critical Rayleigh-number $R_c^{(p)}$, wave number $k_c^{(p)}$ and frequencies ω_c for the onset of oscillatory convection as a function of the initial concentration C_o for the Biot-number B = 1.0, the Soret-number S = -0.0001 and for two values of the latent heat L = 31,3 kJ/kg (solid lines) and 2L (dashed lines).

During the oscillatory convection locally solidification and melting occurs at the interface. Hence, the concentration $\overline{C}^{(L)}(h_L)$ is locally varied. If the oscillations are slow enough to be treated quasi-steadily, this can be interpreted as a change of the effective Sorét number S_{eff}. As was discussed in sections 5b and 5c, an increase of ω_c is to be expected if S_{eff} decreases and strongest variation of ω_c should occur for changes of S_{eff} near S*. This is indeed the case as can be seen from Figs. 10a and 11a.

In summary the numerical results show, that an increased latent heat influences only insignificantly the onset of convection and the wave number but the oscillation frequency of the marginal overstable convection gets noticeably higher for higher values of the heat of fusion.

6. References

Caldwell, D. R.; J. Fluid Mech. 42, 161-175 (1970)

Caroli B., Cardi C., Misbah C., Roulet B.; J. de Physique 46, 401-413 (1985)

Caroli B., Caroli C., Misbah C., Roulet B.;
J. de Physique 46, 1657-1665 (1985)

Chock D.P., Li Chin-Hsiu; Phys. Fluids 18, 1401 (1975)

Coriell S. R., Cordes M. R., Boettinger W. J., Sekerka R. F.; J. Crystal Growth 49, 13 (1980)

Coriell S. R., Sekerka R. F.; PCH Physico Chemical Hydrodynamics 2, 281-293 (1981)

Davis S. H., Müller U., Dietsche C.; J. Fluid Mech. 144, 133 (1984)

Dietsche C., Müller, U.; J. Fluid Mech. 161, 249 - 268 (1985)

Farhadieh R., Tankin R. S.; J. Fluid Mech. 71, 293-304 (1975)

Fischer K. M.; PCH Physico Chemical Hydrodynamics 2, 311-326 (1981)

Foster T. D.; J. Geophys. Res. 74, 6967-6974 (1969)

Guckenheimer J., Holmes P.; Nonlinear Oscillations, Dynamical Systems and Bifurcations of Vector Fields; Springer, New York, 1983; Kap. 7

Hurle D.T.J., Jakeman E.; J. Fluid Mech. 47, 667-687 (1971)

Hurle D.T.J., Jakeman E., Wheeler A.A.; J. Crystal Growth 58, 163-179 (1982)

Hurle D.T.J., Jakeman E., Wheeler A.A.; Phys. Fluids 26, 624-626 (1983)

Hurle D.T.J., Jakeman E.; PCH Physico Chemical Hydrodynamics 2, 237-244 (1981)

Langer, J.S.; Rev. Mod. Phys. 52, 1-28 (1980)

Marshall R.; in: International Conference on Energy Storage, Brighton, April 1981, Vol. 1, p. 129-143

Mihaljan, J.M.; Astrophys. J. 136, 1126-1133 (1962

Mullins W.W., Sekerka R.F.; J. Appl. Phys. 35, 444-451 (1964)

Platten J.K., Chavepayer C.; J. Fluid Mech. 60, 305-319 (1973)

Saitoh T., Hirose K., J. Heat Transfer 102, 261-266 (1980)

Saitoh T., Hirose K.; J. Heat Transfer 104, 545-553 (1982)

Scott M.R.; Watts H.A.; Applied Mathematics Division 2623, Sandia Laboratories, P. O. Box 5800

Sekerka, R.F.; in: Crystal Growth: An Introduction, North-Holland, 403-443 (1973)

Sriranganathan R., Wollkind D.J., Oulton D.B.; J. Crystal Growth 62, 265-283 (1983)

Wollkind D.J., Segel L.A.; Phil. Transactions Roy. Soc. London A 268, 351-380 (1970)

Wollkind D.J., Raissi S.; J. Crystal Growth 26, 277-293 (1974)